Optimized Slag Design for Maximum Metal Recovery during the Pyrometallurgical Processing of Polymetallic Deep-Sea Nodules

David Friedmann[1], Bernd Friedrich[1]

[1]RWTH Aachen University, IME Process Metallurgy and Metal Recycling

Intzestr. 3, 52072 Aachen, Germany

Keywords: Polymetallic Deep-Sea Nodules, Slag Design, Submerged Arc Furnace, Direct Slag Reduction, Thermo-chemical Modelling

Abstract

The steadily growing demand for critical metals and their price increase on the world market makes the mining of marine mineral resources in the not too distant future probable. Therefore, an enormous focus lays currently on the development of a viable process route to extract valuable metals from marine mineral resources such as polymetallic nodules. For a country with few natural resources like Germany, the industrial treatment of marine mineral resources could lead to a significantly decreased dependence on the global natural resource market. The focus during treatment of these nodules lies on the pyrometallurgical extraction of Ni, Cu and Co on one hand as well as the generation of a sellable ferromanganese and/or silicomanganese product on the other. All work is conducted in lab-scale SAF furnaces. The concept approach is zero-waste, which includes careful slag design, so that the produced slags adhere to environmental restrictions.

Introduction

The exploitation of manganese nodules from the deep sea has once again become a political and economic topic in recent years. Many countries have purchased exploration rights for territories in the equatorial pacific ("Clarion Clipperton Zone"; see Figure 1) south of Hawaii from the International Seabed Authority (ISA). The focus of the processing of these nodules lays on the extraction of the industrial metals nickel, copper and cobalt. The nodules would serve as an enormous reserve for these metals, since they are found in relative abundance in many areas in the world's oceans. For example, nodules in the Clarion Clipperton Zone alone constitute an estimated reserve of up to 290 million tons of nickel and up to 60 million tons of cobalt. These estimated amounts currently surpass common land based reserves in mines for nickel, cobalt and manganese [1,2]. Additionally, other valuable metals such as Molybdenum and Vanadium are found in relatively high concentrations.

Much of the current research builds on findings and results from the 1970s [3–5]. Most researches only focus on hydrometallurgical approaches, since energy consumption to dry the $20 - 40\%$ moisture-containing nodules is high. In the 1970s four processes emerged, which were considered viable to extract metal values from ocean nodules [3–6]:

(1) Reductive ammonia leach [7,8]
(2) High-pressure sulfuric acid leach [9]
(3) Reduction and hydrochloric acid leach [10]
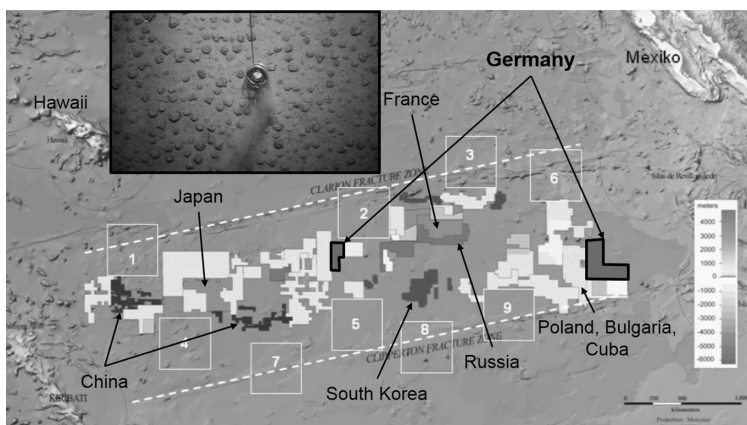(4) Reductive smelting and sulfuric acid leach [11]

Figure 1. Deep-sea nodule exploration license areas to different countries in the Clarion Clipperton Zone in the pacific and impression of nodules on the seabed at 4000-6000 m depth (top). [12]

The research presented in this paper solely focuses on pyrometallurgical processing methods and follows a similar processing route as presented by Sridhar et al. [11,11,13]. A simplified processing scheme is illustrated in Figure 2. The nodules are first dried and pre-reduced in a rotary kiln at 1000°C and charged in to an Electric Arc Furnace. The first reduction step reduces an FeNiCuCo alloy at 1400°C, which is further converted to remove the iron content. The MnO, FeO containing slag is further reduced to produce ferro-manganese. The converter slag may be used to adjust the FeO/MnO ratio in this step. Thus, creating a nearly zero-waste process, if the produced slags are suitable for further use.

More than 95% of the nickel, copper and cobalt are reduced into this metal phase. The alloy only constitutes 6 to 8.5% of the original dry nodule weight. Herein lies the first advantage of a pyrometallurgical processing option. The hydrometallurgical routes struggle with low concentrations of valuable metals in solution after leaching, resulting in complex solvent extraction processes needed to obtain solution suitable for electro winning. In the proposed pyrometallurgical option, the target metals are concentrated by a factor > 20 and may be sold to existing industries. The second main advantage of the pyro route is the production of a sellable manganese product. No hydrometallurgical options generate manganese, which however makes up nearly half of the nodules content (as oxide, moisture free). The chemical composition of nodules from the German license area is given in Table I.

Polymetallic nodules are composed of complex $Mn_xO_y \cdot SiO_2$ and $Fe_xO_y(OH)$ minerals with mineral particles below 1 μm [5]. Ni, Cu, Co and Mo are found in the manganese- or iron-oxide matrix. Therefore, beneficiation with classic techniques (density separation, floatation etc.) to generate a metal bearing concentrate, which could be directly used in existing industries, is not possible making direct metallurgical treatment necessary.
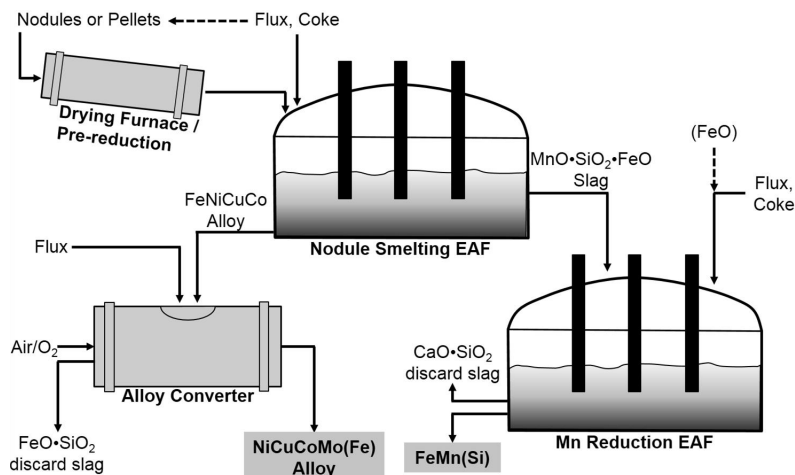
Figure 2. Simplified pyrometallurgical process for the extraction of metal values from polymetallic nodules
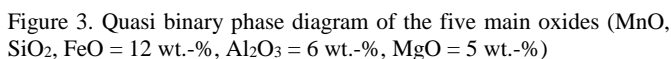
Thermo-chemical Models in FactSage™ 6.4

Thermodynamic models present a great advantage to research of the 1970s and allow the theoretic verification of process routes, which were developed in the past. FactSage™ is a complete thermochemical modelling program with many different applications e.g. phase diagram calculation, thermodynamic chemical reaction calculations, predominance as well as EpH modelling. The Equilib mode uses Gibbs free energy minimization calculations to simulate the reactions of different reactants to reach a state of chemical equilibrium and therefore allows the modelling of phase equilibria. It employs a vast variety of thermodynamic databases of pure substances and solutions. [14]

Table I. Average chemical composition of nodules from the German license area [wt.-%] (wet basis; ~ 20 wt.-% LOI as water)

Mn	Ni	Cu	Co	Mo	V	Fe	Si	Al	Mg	Ca	Zn
31	1.4	1.2	0.16	0.06	0.06	6.2	5.9	2.3	1.9	1.6	0.15
MnO	NiO	CuO	CoO	MoO$_3$	V$_2$O$_5$	FeO	SiO$_2$	Al$_2$O$_3$	MgO	CaO	ZnO
40.02	1.73	1.46	0.20	0.09	0.11	7.98	12.62	4.35	3.15	2.24	0.19

The FactSage™ models consider 15 elements as simple oxides (MnO, FeO, SiO$_2$, NiO, etc.). Trace elements (< 500 ppm) were not taken into account in the calculation to simplify the model. Figure 3 shows the relevant slag system for the first smelting step, a quasi-binary phase diagram of the main oxides is depicted.

Figure 3. Quasi binary phase diagram of the five main oxides (MnO, SiO₂, FeO = 12 wt.-%, Al₂O₃ = 6 wt.-%, MgO = 5 wt.-%)

The x-axis shows the correlation of varying MnO/SiO₂ ratio and resulting equilibrium phases and the liquidus surface. The autogenic slag composition (compare Table I) is also indicated. The model predicts a liquidus temperature of approximately 1540°C, which was verified experimentally in DTA/TGA trials. In the first reduction step (see Figure 2) the main separation of valuable metals from the manganese stream is conducted. However, in a temperature range above 1500°C carbothermic reduction of MnO is significant. This results in high Mn concentrations in the first alloy and subsequently Mn loss for the FeMn reduction, which needs to be minimized.

Silica flux may be added to decrease the liquidus temperature of the slag to values below 1400°C. Different models were created in the "Equilib" mode of FactSage 6.4 to assess silica addition on the first reduction step. The addition of carbon as reductant was varied according to the percentage theoretically needed to reduce all NiO, CuO, CoO, MoO₃ and V₂O₅ up to the quadruple amount needed (~ 29g/kg oxides). The first model with no SiO₂ results in a metal phase with approximately 6.1 wt.-% Mn at 300% C addition. Here the reduction temperature was set at 1650°C (roughly 100°C above liquidus). In comparison, at a MnO/SiO₂ ratio of 1 reduction temperature may be reduced to 1400°C, which results in an Mn content in the alloy of ~2 wt.-%. The target metals Ni, Cu, Co, Mo are reduced with recoveries > 95% at MnO/SiO₂ of 1. Yet, with no flux addition Cu recovery is only about 84%, indicating potential metal loss to the slag. Vanadium is not reduced in this step, but remains in the slag at equilibrium composition. The reduction of iron may not be avoided thermodynamically, resulting in ~ 51 wt.-% in the alloy.

Similarly, the second reduction step of ferromanganese from the resulting slag was simulated and optimized using FactSage™ models. The ratio of $(MnO+CaO)/SiO_2$ (i.e. basicity) was used to characterize the slag. Lime is used to form a calcium silica slag and thus minimize the co-reduction of Si, which is limited for most FeMn qualities to < 1.2 wt.-% [15,16]. Carbon additions were varied as well as the reduction temperature from 1500°C to 1800°C. As expected, Si co-reduction decreases with CaO additions and increases with the temperature. However, Mn reduction recoveries increase with the basicity of the initial slag mixture. Thus a trade-off between undesired Si reduction and maximized Mn recovery.

Experimental Evaluation

All experiments are conducted in a lab-scale DC electric arc furnace, which has a power supply of 50 kW and a melt capacity of 6 liters. The furnace has a water-cooled copper bottom-electrode and a 5 cm diameter graphite top-electrode. The first melting and reduction experiments were conducted in an alumina-chromia castable lining, which proved very stable against the slag and is suitable for temperatures up to 1800°C. The reduction of ferromanganese from the resulting slag was carried out in graphite crucibles.

For the first reduction experiments, nodules were ground (< 0.5 mm) and pelletized with different SiO_2 additions. The pellets were charged into the preheated lab EAF, during charging the furnace was run with an open arc. Once all pellets (~ 3 kg/trial) the graphite top-electrode was submerged into the liquid slag and held for 15 minutes (SAF operation). The solidified slags were broken up, mixed with varying CaO amounts, and charged once again into the preheated graphite crucible. For the reduction in SAF operation the electrode was submerged for 1.5 hours into the slag. During all trials, slag samples were taken in intervals and analyzed via XRF analysis.

Reduction of FeNiCuCo alloy

The alloy predicted in the models makes up approximately 7% of initial oxide input weight. Experimentally, metal weights of 5 to 8% of input weight were obtained, proving thermodynamic models. A phase distribution comparison between FactSage™ models and experimental results is given in Figure 4.
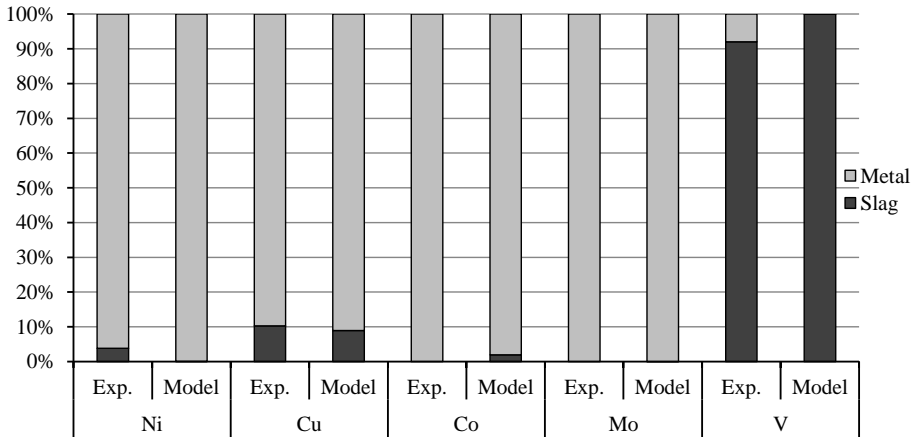

Figure 4. Phase distribution comparison of experimental values and model results (MnO/SiO_2 = 1, at a carbon addition of 200%)

The average metal composition of three different initial slag compositions is given in Table II. As may be seen Mn content in the alloy decreases dramatically when adjusting the MnO/SiO_2 ratio of the slag. Differences in smelting and reduction temperature were also observed and correspond well with liquidus data simulated in FactSage™. The tapping temperature for smelted nodules with no flux addition was between 1600 and 1650°C, whereas tapping temperatures with silica flux could be decreased to values between 1350 and 1450°C.

Table II. Comparison of alloy compositions after the first reduction step [wt.-%]

MnO/SiO_2	Fe	Ni	Cu	Co	Mo	Mn
3.2	54.3	13.4	9.1	0.7	0.5	18.5
2	62.4	17.0	12.7	1.9	0.7	2.2
1	60.4	17.8	10.8	2.0	0.6	2.5

Reduction of FeMn from slag

For the reduction of ferromanganese a slag with 47.4 wt.-% MnO was generated from a larger trail series with an adjusted MnO/SiO_2 ratio of 2 in the first melting and reduction step. The full chemical analysis of the slag is given in Table III. A value for the basicity was established to describe the reduction step:

$$B = \frac{\%MnO + \%CaO}{\%SiO_2} \qquad (1)$$

The autogenic slag possesses a basicity value of 1.63. This highlights the challenge for the FeMn reduction from this slag, when compared to standard manganese ores; whereas the Mn content of the slag is comparable to low-grade manganese ores (B = 3…17) [17], the basicity (i.e. silica content) of the slag is significantly higher (i.e. more acidic). Thereof arises the need for CaO flux to hold Si in the slag.

Table III. Chemical composition of slag for FeMn reduction [wt.-%]

MnO	SiO_2	FeO	MgO	Al_2O_3	TiO_2	CaO	V_2O_5	P_2O_5
47.4	31.0	3.5	4.0	5.1	0.58	3.0	0.11	0.41

Due to limited supply of nodules and therefore limited amount of slag, initially four trials could be conducted. The results are illustrated in Figure 5. The basicity was increased (2.4, 2.6, 2.8 and 3.0) for this trial series. As can be seen from Figure 5 the lowest Mn content in the final slag may be achieved with the highest CaO additions.

The metal phases showed a manganese content of > 85 wt.-% in initial XRF analysis. However, analysis of carbon content is yet outstanding. Fe content in the alloy is ~ 8 wt.-%, which is inside requirements for FeMn. Yet, titanium as well as vanadium content in the reduced metal is problematic with contents ~ 1.3 wt.-% and 0.4 wt.-% respectively. The control of these metals will be subject to further studies. The phosphorous contents on the other hand was not significant and below 0.1 wt.-%. Reduction temperature during SAF operation varied between 1600 and 1800°C as was calculated in the simulations.
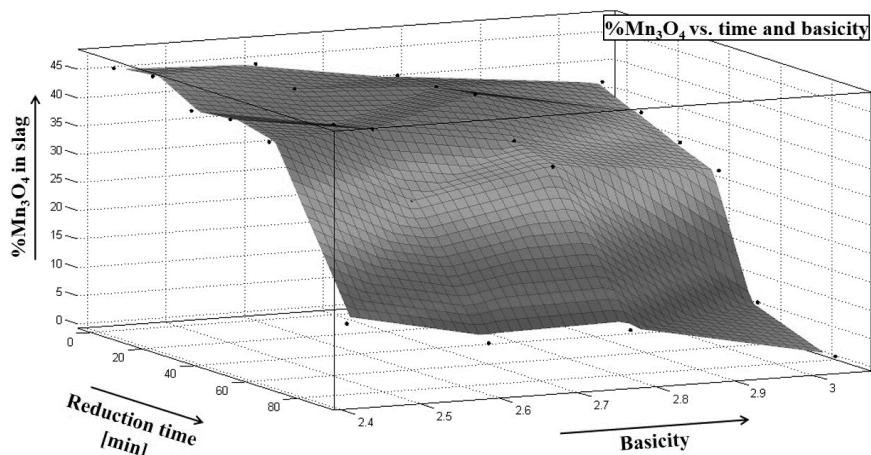
Figure 5. Correlation of Mn content in the slag during reduction versus time (in SAF operation) and basicity

Summary

The first experimental investigation into the described pyrometallurgical process for polymetallic deep-sea nodules were successful. The trials have so far proven the technical feasibility of the process developed mainly in the 1970s. Additionally, this study has shown that there are many advantages of thermodynamic modelling and that it may be used to verify metallurgical processes, which were developed in the past. The FactSage™ models allowed the calculation of the liquidus temperatures of the slag, which were close to experimental data, even though some simplifications had to be made in the models. The metal reduction was also successfully modelled in FactSage™ and the results could be proven in the experiments. Overall, it could be shown that by careful adjustment of the MnO/SiO$_2$ ratio it is possible to separate most of the manganese content of the nodules from metal values (i.e. Ni, Cu, Co). The use of an electric arc furnace to melt and separate the two phases has many advantages and could be easily adapted to an industrial scale.

The initial experiments on the reduction on ferromanganese from the slag produced in the first reduction step showed that the production of a sellable manganese product from deep-sea nodules is possible. However, further studies are needed to adjust the slag to produce FeMn that adheres to FeMn standards. The option of the production of SiMn as well as FeMn in a two-stage reduction step will also be investigated. Additionally, further studies on the entire process are planned in the future since the investigation of the conversion of the FeNiCuCo alloy is outstanding. Furthermore, a scale-up of the process from lab-scale is planned.

Overall, the advantages of the pyrometallurgical processing route compared to hydrometallurgical options are described and proven by the experimental trails. The valuable metals are easily separated and concentrated from the manganese stream. The advantage of the production of a manganese product from polymetallic deep-sea nodules are also outlined. However, the exploitation of these nodules remains a political topic, but could offer decreased dependency on raw material imports, which will be especially important for raw material import-dependent countries like Germany.

References

1. R. K. Jana, "Processing of Polymetallic Sea Nodules: An Overview," *The proceedings of the Third ISOPE Ocean Mining Symposium* (1999), 237–245.
2. J. Lehmköster, N. Gelpke, and M. Visbeck, *World Ocean Review 3 (www.worldoceanreview.com): Resources of the sea - chances and risks* (Hamburg: maribus gGmbH, 2014).
3. P. Halbach, G. Friedrich, and U. von Stackelberg, *The Manganese Nodule Belt of the Pacific Ocean* (Stuttgart: Ferdinand Enke Verlag, 1988).
4. G. L. Hubred, "Manganese Nodule Extractive Metallurgy Review 1973 - 1978," *Marine Mining*, 1980, no. 3:191–212.
5. U.S. Bureau of Mines, "Pacific Manganese Nodules: Characterization and Processing (Bulletin 679)" (Bulletin 679, U.S. Bureau of Mines, 1985).
6. K. N. Han, and D. W. Fuerstenau, "Metallurgy and Processing of Marine Manganese Nodules," *Mineral Processing and Extractive Metallurgy Review: An International Journal*, 1983, Vol. 1:1–83.
7. J. C. Agarwal, and T. C. Wilder, *U.S. Patent 3788841: Recovery of metal values from manganese nodules*, 1974.
8. J. C. Agarwal, N. Beecher, and D. S. Davies, "Processing of ocean nodules: A technical and economic review," *Journal of Metals (JOM)*, 1976, Vol. 28 No. 4:24–31.
9. K. N. Han, and D. W. Fuerstenau, "Acid leaching of ocean manganese nodules at elevated temperatures," *International Journal of Mineral Processing*, 1975, no. 2:163–171.
10. P. H. Cardwell, and W. S. Kane, *U.S. Patent 3950486A: Method for separating metal constituents from ocean floor nodules*, 1976.
11. R. Sridhar, W. E. Jones, and J. S. Warner, "Extraction of copper, nickel, and cobalt from sea nodules," *Journal of Metals (JOM)*, 1976, Vol. 28 No. 4:32–37.
12. Federal Institute for Geosciences and Natural Resources, Manganese nodule exploration in the German license area. www.bgr.bund.de.
13. R. Sridhar, "Thermal Upgrading of Sea Nodules," *Journal of Metals (JOM),* 1974 (12) (1974), 18–22.
14. C. W. Bale et al., "FactSage thermochemical software and databases," *Calphad,* 26 (2) (2002), 189–228.
15. ASTM International, *(A99-03) Standard Specification for Ferromanganese*, 2 pp. (accessed 25 June 2015).
16. DIN Deutsches Institut für Normung e.V., *(DIN 17564) Ferromanganese, Ferromanganese-Silicon and Manganese – Technical delivery conditions*, 6 pp., 2004 (accessed 29 January 2016).
17. F. Habashi, ed., *Handbook of Extrative Metallurgy* (Wiley VCH, 1997).

Acknowledgments